THE BELL SYSTEM TECHNICAL JOURNAL
Vol. 56, No. 10, December 1977
Printed in U.S.A.

WT4 Millimeter Waveguide System:

Mechanical Design of Sheathed Waveguide Medium

By R. W. GRETTER, R. P. GUENTHER, M. LUTCHANSKY, D. OLASIN, and A. B. WATROUS

(Manuscript received April 7, 1977)

The mechanical design of the sheathed waveguide medium for the WT4 System provides means for the fusion joining of waveguide modules into a continuous transmission line and for limiting the distortions added by the joining and installation processes. In addition the fusion-joined steel sheath guarantees a much higher degree of protection for the medium than is present in any of the existing long-haul transmission lines. A summary of the development program of the sheathed waveguide medium used in the recent field evaluation test is presented herein. Results are given of the study conducted to establish the welding procedures used and steps in the evolution of the welded coupling design are reviewed. A discussion is given of the behavior of the two-stage mechanical filter that attenuates the effects of the irregular soil forces acting on the sheath. Estimates of the field test losses attributable to the joining and installation processes are also given.

I. INTRODUCTION

1.1 Sheathed medium components

The installed WT4 transmission medium is composed of four basic mechanical elements; the outer sheath, supports for the waveguide within the sheath, the waveguide couplings, and the cylindrical waveguide tubing (Fig. 1).

The outer sheath is a steel pipe manufactured by conventional methods and coated with a layer of polyethylene extruded over a black mastic undercoating. In addition to filtering the effects of irregular earth forces on the installed medium, the sheath affords protection for the

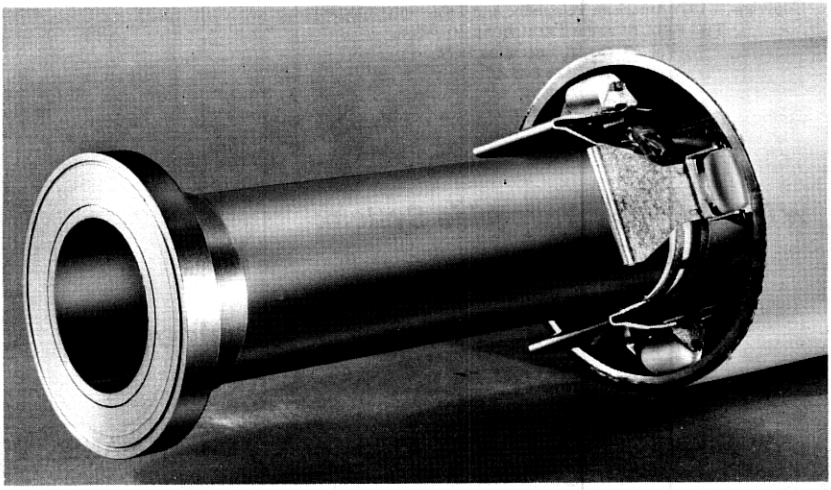

Fig. 1—Components of WT4 sheathed waveguide medium.

waveguide against lightning, corrosion, damage by "foreign" workers, and other hazards.

The roller-spring supports shown in Fig. 1 permit axial motion of the waveguide in the sheath with very low friction. The compliance of the supports in conjunction with the stiffness of the waveguide tubing provides a mechanical filter with respect to the influences, on the waveguide curvature, of the sheath surface distortions as well as the irregularities in the supports themselves.

The couplings, which are all fusion-joined, provide for accurate alignment and reliable connection of the waveguide sections.

The design, fabrication, and characterization of the waveguide tubing are discussed in companion papers by Boyd, et al.[1] and Thomson[2]. This paper covers mechanical design considerations for the other elements of the installed medium and the effects of these elements on transmission losses.

1.2 Transmission constraints on the mechanical design

Electrical transmission considerations establish a number of mechanical design constraints. Both the magnitude and distribution, along the length, of geometric imperfections (deviations from the geometry of a right circular cylinder) in the WT4 waveguide medium are of importance. It has been shown by Rowe and Warters[3] that, for small continuous imperfections in dielectric-lined waveguide, the expected values of average mode conversion losses, from the primary TE_{01} mode, are proportional to the power spectral density levels of the imperfections.

Aside from diametral distortions in the vicinity of the waveguide coupling, imperfections associated with joining and installation are in the form of variations of axis curvature. The most important curvature-coupled spurious modes are the TM_{11} and TE_{12} which, in the 40 to 110 GHz operating frequency range of the field-test system, are produced by high levels of Curvature Power Spectral Density (CPSD) in the 0.3 to 1.5 c/m (cycles per meter) mechanical-frequency range. It is shown in a companion paper by Carlin and Moorthy[4] that significant amounts of loss to the TM_{21} mode can occur for relatively large CPSD amplitudes in the low mechanical-frequency range ($f < 0.15$ c/m). The sheathed medium is an effective mechanical filter with respect to inputs above 0.15 c/m whereas control of the low mechanical-frequency range is a matter of trench design and trench bottom quality, as is discussed in the companion paper by Anderson et al.[5] The present paper deals with inputs associated with waveguide assembly and installation and the action of the sheathed medium in limiting waveguide CPSD levels, particularly in the range of coupling of TE_{01} to the TM_{11} and TE_{12} modes.

II. MECHANICAL FILTERING

2.1 Flow diagram

The WT4 sheathed medium provides two stages of mechanical filtering, one being the sheath stiffness which aids in smoothing the effects of loading irregularities imposed by the surrounding soil, and the second the waveguide stiffness in combination with the waveguide support compliance. The two stages can be considered as independent because the sheath and waveguide are installed in separate operations. Both stages are low-pass filters. A number of inputs influence the net waveguide curvature as indicated in the flow diagram of Fig. 2. The input and output lines of the diagram have been given profiles which roughly illustrate their spatial variations. The trench bottom roughness and soil forces are acted upon by the sheath filter producing the smoothed response referred to in the figure as the "sheath burial curvature." As Fig. 3 illustrates, the sheath makes only partial contact with the trench bottom and therefore its filtering characteristics are nonlinear, depending on the soil loading as well as its own parameters. Other contributions to the net sheath curvature are the imperfections in the sheath splices, in the form of tilts and offsets, and imperfections in the sheath as manufactured.

The deformations in the installed sheath surface act as inputs to the bases of the spring supports. Since nonuniformities in the heights of the springs have the effects of displacements of the spring bases, they are summed with the sheath displacements to give the total input to the next stage of filtering. The output of the second stage, referred to as the

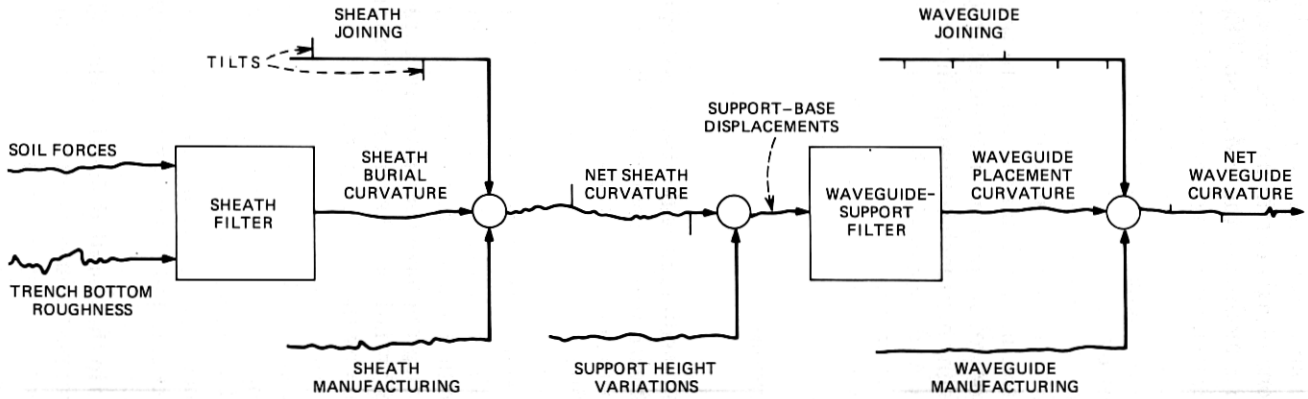

Fig. 2—Waveguide curvature inputs and filtering.

"waveguide placement curvature," reflects all of the deleterious effects of installing a joined string of waveguide sections. To this are added the waveguide manufacturing and joining imperfections to produce the "net waveguide curvature." A conservative simplification is made in this model by assuming that the joining and manufacturing inputs by-pass the filters. Both stages actually behave as high-pass filters with respect to these imperfections, whose low mechanical-frequency content is generally negligible relative to that of the other inputs. Because of the influence of the second-stage filter, tolerances on the sheath and supports are much less stringent than the tolerances associated with the waveguide manufacture and joining. Conversely the waveguide joining imperfections are potentially significant contributors to the higher mechanical frequency portions of the net waveguide CPSD. Achieving the necessary precision in the couplings was recognized at an early stage as a particularly challenging objective.

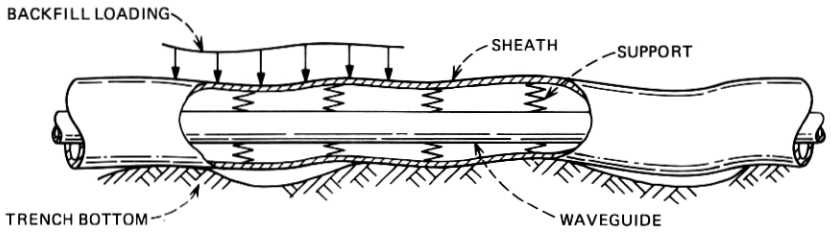

Fig. 3—Two-stage mechanical filter.

2.2 Waveguide CPSD components at 0.325 c/m

The most critical mechanical wavelength is the beat wavelength of the TE_{01} and TM_{11} modes at the highest frequency in the operating band. The mechanical frequency associated with 110 GHz is 0.325 c/m for the dielectric-lined waveguide used in the WT4 field test. Estimates of the various components of the net waveguide CPSD will be given below. Using field test data it was found that the sheath burial, support irregularities, and sheath joining each accounted for contributions to the waveguide CPSD at 0.325 c/m in the order of 10^{-8} l/m^2/c/m while the contributions of sheath manufacturing and waveguide joining were at least an order of magnitude lower. The sum of all of these contributions corresponds to an expected value of average TM_{11} mode conversion loss, at 110 GHz, of less than 0.05 dB/km which is well within acceptable limits for a practical system.

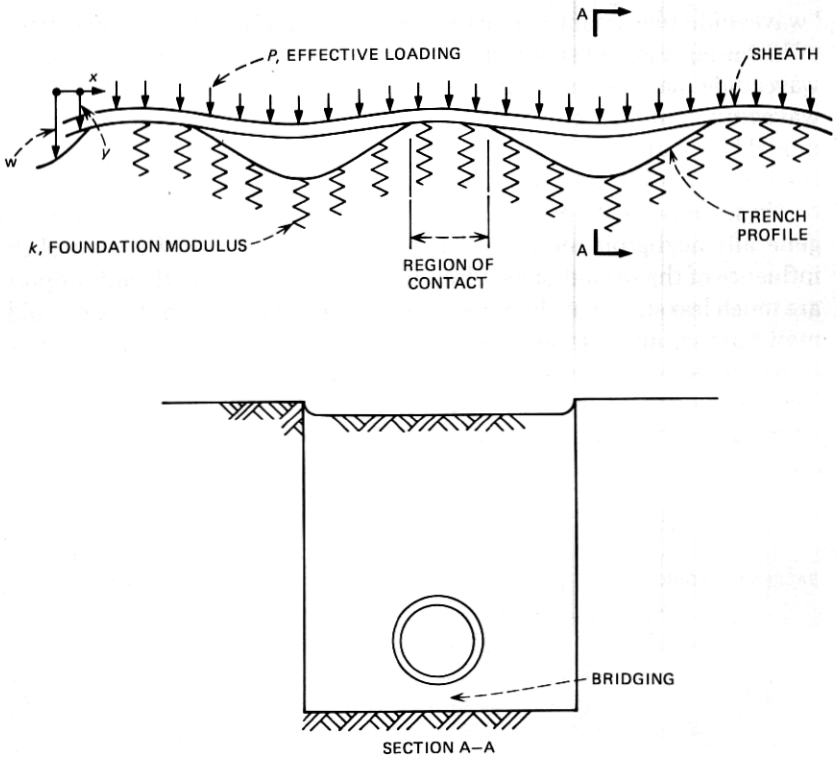

Fig. 4—Sheath-soil interaction model.

2.3 Sheath filtering

2.3.1 Mathematical model

For purposes of understanding the filtering action of the sheath on the soil environment, a mathematical modeling investigation was carried out. The modeling is useful in investigating the effects of trench bottom irregularities as well as sheath parameter and loading variations. The essential features of the sheath deformation process are described by a beam-on-elastic-foundation model where the free surface of the foundation is taken to have the irregular shape of the as-cut trench bottom. The trench bottom is taken to be a continuous elastic foundation of the Winkler type—i.e., composed of an infinite number of independent linear springs of differential width. The beam is assumed to respond to a known loading which reflects not only the weight of the sheath but the effective weight of the backfill.

Referring to Fig. 4, the governing equations for the beam resting on an irregular surface with only partial contact existing are as follows

$$EIy^{IV} = p \qquad y < w \tag{1}$$

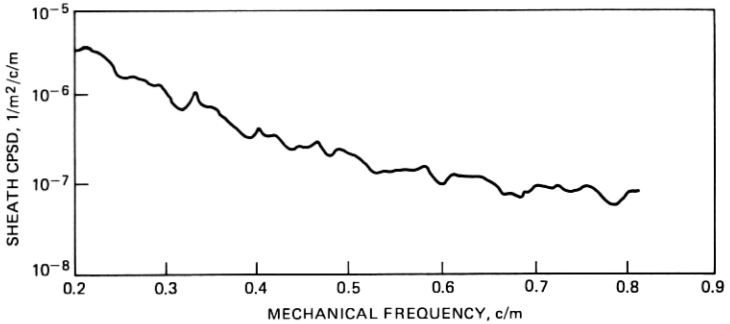

Fig. 5—Average of sheath curvature spectra for field evaluation test.

and

$$EIy^{IV} + ky = p + kw \qquad y \geq w \tag{2}$$

where y is the beam deflection, w is the vertical distance from a horizontal reference line to the soil surface, E is Young's modulus of the sheath material, I is the sheath cross-sectional moment of inertia, k is the foundation modulus, and p is the loading per unit length. Because the regions of contact in which eq. (2) applies are not known in advance, an iterative procedure is required to obtain a solution starting from an initial guess as to where contact exists. A finite difference method was employed to obtain solutions of these equations for trench profiles of arbitrary shape. The computer program written for the sheath analysis was used in obtaining curvature estimates with trench profile data from the field test installation.

2.3.2 Field test results

Figure 5 shows a CPSD estimate obtained using field-test trench profile data. The steel sheath dimensions are $5^9/_{16}$ inch outside diameter and $^3/_{16}$ inch wall thickness. A loading of 8 lb/in. was assumed, which reflects some conservatism as discussed below. The CPSD estimate was obtained by averaging, at each mechanical frequency, sample spectrum values from 12 data sets, each representing 300 feet of trench.

Results of the sheath analysis showed the sheath filtering to be virtually unaffected by the actual value of foundation modulus for typical values ($k > 5000$ lb/in.^{2}).

2.3.3 Sheath loading

Estimates of the loading which was effective in producing bending of the sheath axis were obtained from a limited experimental program. Figure 6 shows some results of these experiments in which deflections were measured for simply supported 20-foot lengths of sheath buried

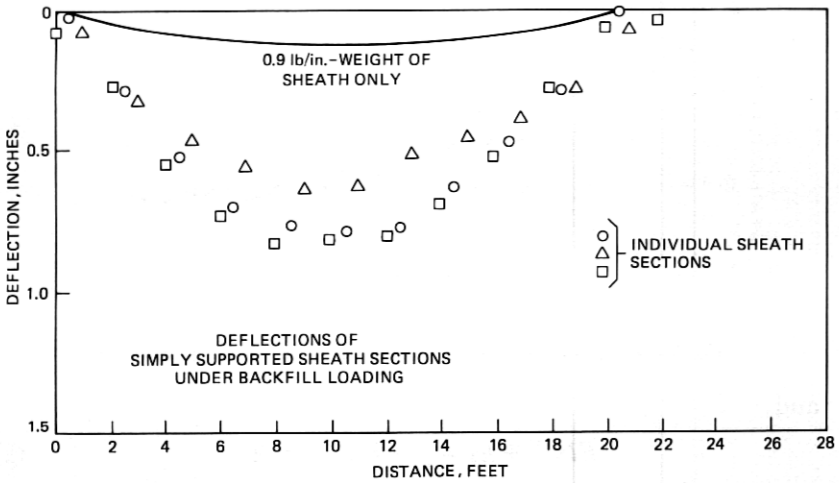

Fig. 6—Experimental determination of effective sheath loading.

in a manner typical of pipeline construction. An effective loading of between 4 and 6 lb/in. was estimated from these tests (about a third of the weight of the backfill directly above the sheath plus the weight of the sheath). As noted above, a somewhat higher loading (8 lb/in.) was used for estimating losses to allow for field conditions not encountered in the experimental installations. It should be noted that the effective sheath loading, referred to here, is a downward beam loading. It is not the same as the crushing loads used in the two-dimensional analysis of uniformly supported buried conduit (cf. Spangler[6]).

2.4 Waveguide-support filtering

2.4.1 Transfer function

The waveguide support within the sheath consists of a set of relatively closely spaced spring elements. The filtering mechanism is very nearly like that of the continuum model of a beam on an elastic foundation as described in the previous section. Here the springs are attached to the beam and the inputs are deflections of the bases of the springs. Because an interference fit between the supports and sheath would increase the effective coefficient of friction for insertion, a slight clearance is allowed. This is ignored in assessing the filtering behavior as the effect is small considering the relatively large amplitude, long wavelength content of the trench profiles observed. Thus, the waveguide-support system is regarded as a linear filter described by eq. (2), if axial loads are ignored. Here w represents the deflections of the bases of the springs.

It is assumed in eq. (2) that the slope of the elastic curve is small everywhere and, accordingly, the waveguide curvature

$$C_g \approx y_g^{II} \tag{3}$$

so that for a uniformly loaded beam having a uniform foundation modulus

$$EI_g C_g^{IV} + kC_g = kC_s \tag{4}$$

where C_s is the curvature of the envelope of the spring bases. The transfer function with respect to sinusoidal input components is

$$H(\omega) = \frac{1}{1 + \dfrac{EI\omega^4}{k}} \tag{5}$$

where $\omega \equiv 2\pi f$.

The CPSD function of the waveguide, S_o, caused by sheath curvature is determined using the input-output relation for linear systems

$$S_o(\omega) = |H(\omega)|^2 S_i(\omega). \tag{6}$$

The parameters used in the WT4 system are: $E = 30 \times 10^6$ lb/in.^{2}, $I = 0.94$ in.^{4}, and $k = 20$ lb/in.^{2} The squared gain function $|H(\omega)|^2$, is shown in Fig. 7 along with the range of mechanical frequencies associated with TE_{01}–TM_{11} and TE_{01}–TE_{12} mode conversion. The magnitude of $|H(\omega)|^2$ is less than 0.01 in the critical range and falls off as the eighth power of mechanical wavelength (24 dB per octave). Because of this high cutoff rate, the design criteria for the inputs acted on by this filter (Fig. 2) are simplified. For all these inputs, peak mode-conversion effects occur at the high end of the operating frequency range with TM_{11} more significant than TE_{12}, although TE_{12} has larger coupling coefficients.[4] Thus a useful figure of merit for assessing the various loss contributions is the CPSD level at a mechanical frequency of 0.325 c/m which, as mentioned earlier, corresponds to TE_{01}–TM_{11} coupling at an operating frequency of 110 GHz for the field test waveguide (180 micron dielectric liner thickness).

Deviations from the continuum filtering behavior occur in two ways as a result of the discrete nature of the supports. Because the supports "sample" the sheath internal surface, aliasing phenomena are present. Also, because the loading impressed on the waveguide is actually a set of discrete forces, the waveguide response to a sinusoidal distortion in the sheath contains response components at shorter wavelengths as well as at the same wavelength as the sheath input. For the 22-inch support spacing used and the field test input data, these deviations have been found negligible.

If an axial force, T, is present in the waveguide, a second-order term

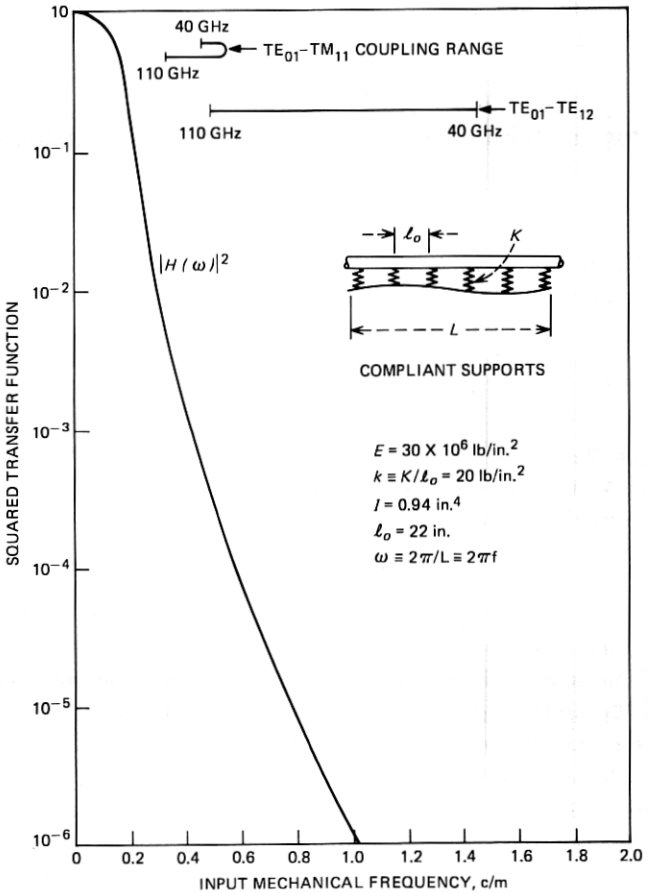

Fig. 7—Response of waveguide-support system.

is added to the left side of eq. (4) and the transfer function is modified to

$$H_T(\omega) = \frac{1}{1 + \frac{T\omega^2}{k} + \frac{EI\omega^4}{k}} \tag{7}$$

The axial force due to temperature fluctuations, with no expansion joints, can be either positive (tensile) or negative (compressive). Adding the axial load, which may reach levels in the order of 10,000 lb, changes the magnitude of the transfer function by less than 15 percent for a 10-foot wavelength input, and by smaller amounts for shorter mechanical wavelengths.

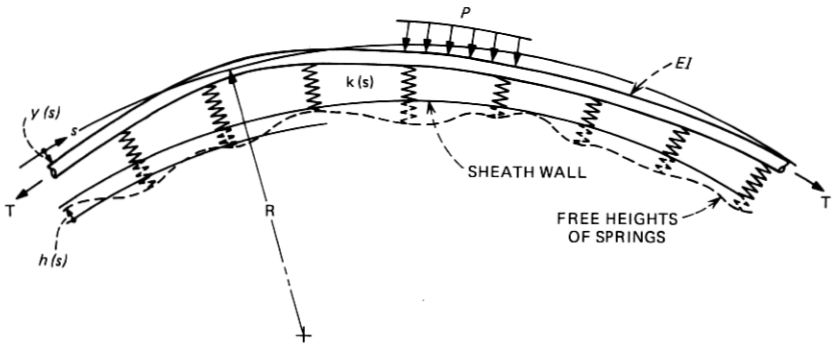

Fig. 8—Effects of support irregularities.

By selecting the support spacing sufficiently small, the mechanical wavelengths of distortions caused by waveguide weight and thermal loading were placed outside the critical range. The shortest wavelength in the range is 27 inches. Buckling of the waveguide under compressive loading is not a problem because the critical buckling load for the WT4 support parameters is in excess of 47,000 lb, which is much greater than any loading anticipated.

2.4.2 Roller-spring support irregularities

Irregularities in the supports are of two types: spring constant variations and variations in the free heights of the supports. The effects of the spring constant variations are only of significance under conditions in which the supports are highly compressed. This occurs when a high axial force exists in the waveguide in a curved region of the trench, as shown in Fig. 8. The waveguide is assumed to be loaded by an axial force, T, which is the result of a temperature variation from that corresponding to a stress free state, and a transverse loading, p, which represents the weight if the curvature is in the vertical plane. (It is assumed that slopes in the vertical plane are sufficiently small that no distinction is needed between the weight and its radial component. Also, changes in T due to the tangential components of weight or frictional effects are ignored.) The radius, R, is taken as constant here because the support variations are much more rapid than the local average curvature. Dropping the subscript g, the waveguide deflection, $y(s)$, is a displacement from the curved reference line. The governing equation is then

$$EI\left[y(s)^{IV} + \frac{1}{R^2}y^{II}\right] - Ty^{II}(s) + k(s)y(s) = \left[p + \frac{T}{R}\right] + k(s)h(s) \quad (8)$$

where $h(s)$ is the variation in the free height of the spring taken positive when the height is less than nominal, and $k(s)$ is the variation in spring constant due to material thickness variations in the roller spring supports and the effects of sliding friction as the support is compressed. Equation (8) reduces to eq. (2) for a uniform support in a nominally straight section of trench and with zero axial force.

An approximate solution of eq. (8) may be obtained by a perturbation technique, putting the spring constant and height variations in the form

$$k(s) = k_o + \epsilon f(s)$$

and

$$h(s) = \epsilon q(s)$$

where ϵ is a small parameter and $f(s)$ and $q(s)$ are assumed to be stationary stochastic processes with zero averages. By expanding the solution in a power series in ϵ and retaining the first two terms the approximate solution is obtained. The waveguide CPSD approximation due to the support irregularities can be expressed

$$S_{ir}(\omega) \approx \omega^4 |H_T(\omega)|^2 \left[S_h(\omega) + \frac{\hat{p}^2}{{k_o}^4} S_{\bar{k}}(\omega) \right]$$

where $S_h(\omega)$ is the spectrum of the height variations, $S_{\bar{k}}(\omega)$ is the spectrum of the spring constant variations, and the two types of variations are taken as independent. The loading parameter

$$\hat{p} \equiv p + T/R$$

It was found that the field test support data could reasonably be represented as band-limited white noise and the corresponding waveguide CPSD approximation in the critical range is

$$S_{ir}(\omega) = \omega^4 |H(\omega)|^2 \times 10^{-7} \qquad 1/\text{m}^2/\text{c}/\text{m} \qquad (9)$$

where ω is in radians/meter and the effect of the axial tension in the transfer function is ignored.

2.4.3 Design considerations for the roller-spring supports

The roller-spring support has two basic functions; to facilitate insertion of the waveguide and to act, in conjunction with the bending stiffness of the waveguide, as a mechanical filter. Since a relatively large number of supports is required, feasibility of the support system is dependent on low unit costs, ease of attachment to the waveguide and high reliability. Fulfilling the insertion objective was primarily a matter of selecting appropriate materials. The roller material chosen is a 30 percent glass-filled nylon and the axle pins are 303 stainless steel coated with

a thin fluorocarbon film. The glass reinforcement provides adequate strength to guarantee dimensional stability of the rollers under the anticipated long-term loading. The effective average coefficient of friction is sufficiently low to permit insertion of the waveguide up to 3 miles from a single push site as discussed in the companion paper by Baxter et al.[7] Very little wear has been observed in testing these rollers for simulated insertion distances far exceeding 3 miles.

The low-cost objective is met by the WT4 roller-spring support (Fig. 9). The carriage for the rollers is a one-piece sheet-steel part incorporating its own attachment clip. The blank is formed into four bow-tie shaped springs by punch-press operations and is made from steel of relatively high ductility as well as high yield stress. Heat-treatment is not required to achieve the necessary spring temper, and design is such that the support may be mass-produced in a completely automated punch-press process. It is estimated that in mass production the cost of a complete assembly will be less than 60 cents. The sheet material is corrosion protected with a zinc coating.

The requirements for the filter are to provide sufficient compliance to achieve adequate attenuation of inputs in the critical mechanical frequency range. The initial objective was to achieve a squared transfer function magnitude of 0.01 or less at a mechanical frequency of 0.325 c/m. For the 20 lb/in.^{2} average support modulus obtained, the value of the squared transfer function is about 0.008 at that frequency. As can be seen from eqs. (5) and (6), the attenuation of spectral inputs is proportional to the square of the spring stiffness. The lower limit on spring stiffness is determined by the reactions to the thermal loading that must be developed within the elastic range of spring deflection and by the geometric constraints within the sheath.

The maximum allowable elastic range of deflection of the supports is less than the radial clearance between the coupling flanges and the sheath inside surface. In the field test waveguide this distance is nominally a little over half an inch. Under the peak lateral loads due to thermal forces, the supports must have some elastic travel remaining for filtering. In the field test supports the transverse loading corresponding to a 10,000-lb axial force in a 250-foot radius route bend displaces the axis of the guide about 75 percent of the elastic range of the supports, which is a little under $\frac{1}{4}$ inch. Supports made since the field test using a newly available steel of higher yield strength has increased this range, for the same support design, by about 25 percent.

To obtain high efficiency in the spring design the supports utilize the increased elastic range of travel available when the support is allowed to deflect well beyond its elastic range during its first loading. For elastic, perfectly plastic materials, the maximum load is up to 1.5 times that for a flat spring loaded only up to yielding of the outer fibers. Although the

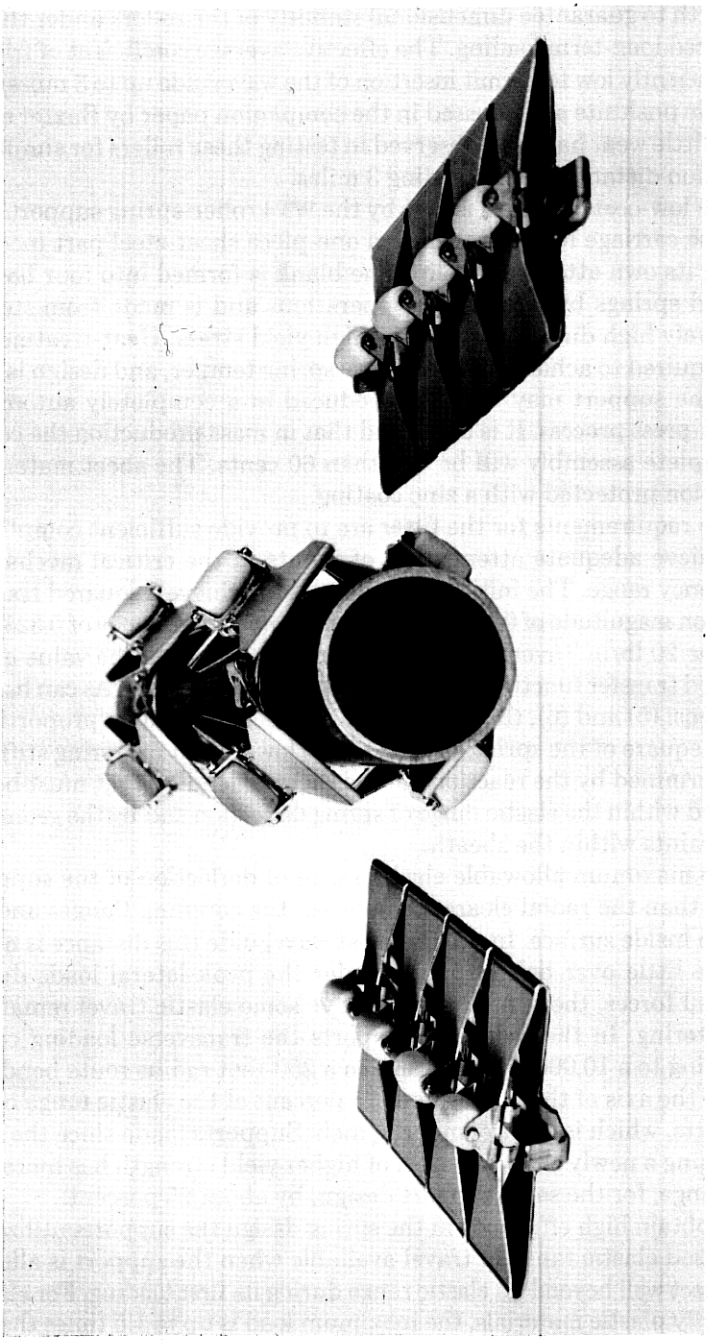

Fig. 9—Roller spring supports.

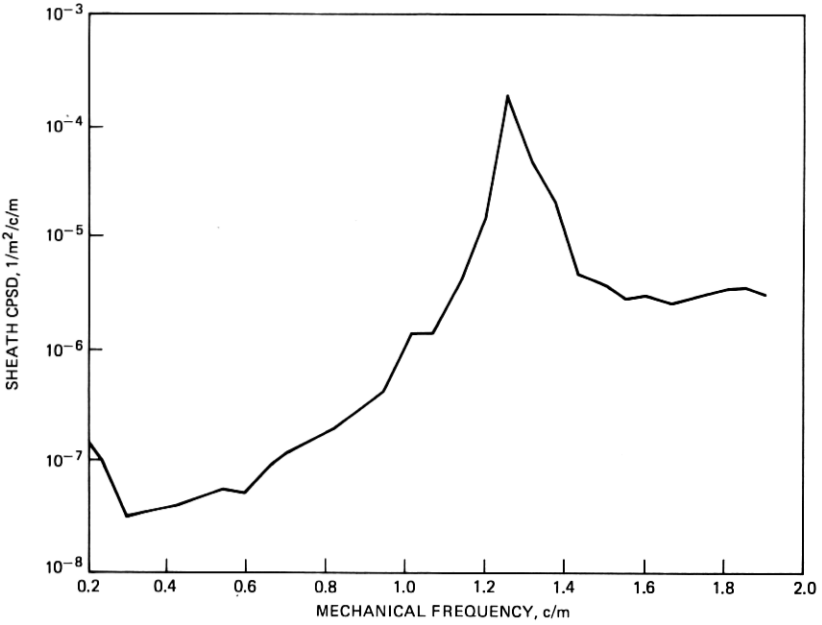

Fig. 10—Average of CPSD plots.

load-deflection curve is somewhat nonlinear during first loading, it is nearly linear on subsequent loadings. In future applications the supports will be subjected to one full deflection in the factory during module preparation. This was not done for the field test modules; therefore more care was required in handling them to prevent changes in the free heights of the springs.

III. SHEATH CONSIDERATIONS

3.1 Manufacturing irregularities

The size and material requirements of the sheath are met by commercially available standard line pipe. To control the effects of sheath manufacturing curvatures on the net waveguide curvature, the specification of sheath straightness tolerance is in terms of an allowable power spectral density limit. The sheath for the field test was inspected using an external curvature gauge, the principles of which are described in the companion paper by Fox et al.[8] Figure 10 shows an average of CPSD plots obtained from 30 of the 60-foot-long field test sheath sections. The relatively high spectrum spike at 1.25 c/m was the result of an eccentricity in a set of sizing rollers through which the sheath passed during manufacture. It is above the "cutoff" frequency of the discrete waveguide supports and is thus aliased by the supports to appear as an input at 0.55

c/m. The amplitude of the effective input spike at 0.55 c/m is reduced in magnitude by the fourth power of the ratio 0.55/1.25 and thus its effect is quite small.

3.2 Sheath joining irregularities

Because, when sheath sections are joined, mating ends are butted together, the magnitude of sheath splice tilts is primarily determined by the out-of-squareness of the sheath ends. A tilt may be considered a delta function in curvature and the curvature power spectral density for a set of equally spaced random tilts in one plane has the simple form[3]

$$S_{t_1}(\omega) = \sigma_t{}^2/L \tag{10}$$

where L is the sheath section length and $\sigma_t{}^2$ is the variance of the tilt magnitudes. Assuming random angular orientations of joining members

$$S_{t_1}(\omega) = \frac{E(A^2)}{L} \tag{11}$$

where $E(A^2)$ is the mean square out-of-squareness of the sheath ends with respect to a plane perpendicular to the sheath axis.

An additional contribution to the tilt may occur if the sheath end faces are not perfectly butted together. The amount of gap allowed by the sheath welding specification was 0.01 inches, which limited this contribution to a negligible level. Using the field test sheath end-squareness data an estimate of the effective tilt spectrum for two orthogonal planes is

$$S_t(\omega) = 9 \times 10^{-7} \quad 1/\text{m}^2 \tag{12}$$

The offsets at sheath joints are characterized as a set of delta functions in slope. Thus the offset curvature power spectral density for one plane is

$$S_{o_1}(\omega) = \frac{\omega^2 \sigma_o{}^2}{L}$$

where σ_o is the standard deviation of offset. From the specified tolerances on wall thickness it can be concluded that the sheath offset contribution is negligible.

3.3 Sheath welding

The sheath welds provide gas-tight joints and sufficient strength for sheath handling. Because the inside surface of the sheath serves as a

runway for the rollers during insertion, it was felt necessary to utilize a weld that created no projections on the inner surface.

The field test sheath sections were joined by SMA (Shielded Metal Arc) welding, a manual process. Other processes are available which can be used satisfactorily for this application. The type of joint selected for the field test differs from standard pipeline practice in that the mating sheath ends are butted together, completely closing the gap, with the weld beads penetrating sufficiently deep to achieve the required joint strength for pipe handling while not completely penetrating to the inner surface. Use of a partial rather than a full penetration weld and zero (nominal) gap between mating ends are the only differences from standard pipeline practice. The sheath wall thickness ($^3/_{16}$ inch) was selected to be the smallest practical value. Thinner-walled pipe could not be reliably joined by butt welding without requiring the use of undesirable reinforcing rings. In addition the thinner-walled pipe is much more prone to denting due to mishandling.

A two-pass weld procedure was used for each splice. The first relatively-thin "root" or "stringer" pass is followed by a final pass using a lateral weaving technique, building up a heavy weld bead on the outer surface. Strength is achieved in this joint nearly equal to the strength of the pipe body. Approximately 750 welded sheath joints were made for the field test with only one failure, which was detected and repaired after completion of the installation.

IV. WAVEGUIDE COUPLING

4.1 Requirements

The waveguide coupling consists of flanges (Fig. 1) that are EB (Electron-Beam) welded to the waveguide tube in the factory and fusion-joined in the field by TIG (Tungsten Inert-Gas) welding, a machine process. The specifications developed to assure reliable joining and satisfactory transmission performance for the coupling are given in Table I.

An all-fusion joined coupling was selected as the joining approach for waveguide modules, primarily because of reliability considerations. An extensive analytical and experimental program, which can be discussed only briefly here, was carried out to develop the coupling.

4.2 Coupling design

The waveguide flanging process (Fig. 11) starts with the machining of flange blanks from forgings or heavy-wall tubing. The material chosen for the flange blanks is aluminum-killed low-carbon (C1010) steel, a choice based on TIG welding requirements.

Table I — Coupling specifications

Item	Requirements	Rationale
Strength (tensile)	1. 40,000 lb min. failure load 2. 100 cycles from 0 to 35,000 lb 3. No yield below 30,000 lb	40°F temp change in 250 ft bend, 2 to 1 safety factor
Leakage (maximum)	1. Average 5×10^{-5} cm^3/sec 2. Max. 1×10^{-3} cm^3/sec	Leak location required in N_2 system
Permeability	(Requirement not necessary with fusion joining)	
Tilt	0.2 millirad rms maximum	Loss objective
Offset	2.0 mils rms maximum	Loss objective
Excess stiffness	No requirement	Optimized after all other requirements met
Diametral distortion	2.0 mil max. at coupling	Loss objective

The shape of the flange was determined at an early stage of the coupling development using finite element analyses. A flange diameter of slightly over 4 inches was found adequate to keep the temperature of the dielectric liner below 250° F (a material requirement) during the TIG welding in the field.

Although the basic flange shape changed little during the latter part of the development, several flange face variations were investigated in an effort to facilitate welding. The large grooves in flange face designs 1, 2, and 3 of Fig. 12 led to pressure-vessel effects (weld blow-out) during the TIG welding process. Flange 4 did not meet strength requirements because of the stress concentration at the TIG weld. Flange 5, which incorporates a small stress relief groove, satisfies both the welding and strength requirements and is the design used for the field test.

The face design of flange 6 has an undercut which is made during the blank machining process. This design is proposed for the next generation of waveguide flanges because it minimizes the final machining effort and eliminates machining the hard martensitic steel region near the electron-beam face weld.

The TIG fusion-joining process uses a specially designed fixture that aligns the flanges, clamps them together with a 10,000-lb preload, rotates the welder head around the coupling, and cools the coupling by means of water-cooled copper heat sinks pressed against the flanges. The preload minimizes the separation of the flange faces when the waveguide is in tension or bending. The welding parameters are critical and are given in Table II.

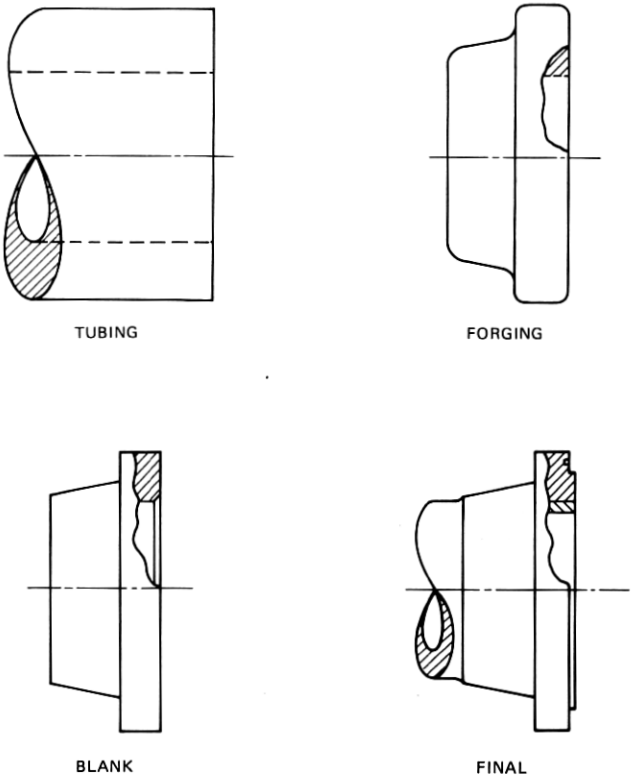

Fig. 11—Flanging process.

4.3 Coupling—field test reliability results

The coupling used in the field test waveguide met or exceeded all of the reliability objectives. Tests demonstrated that:

(*i*) The coupling exceeded strength requirements and is satisfactory for use in bends with radii of curvature as low as 180 ft.

(*ii*) The coupling is very insensitive to stress corrosion cracking.

(*iii*) The 8.7 mile waveguide string, containing over 1500 couplings, has no measurable nitrogen leakage.

The welding process proved to be extremely reliable with only one defective weld, which was easily replaced, out of the over 1500 produced during the field test. Inspection of the welds was visual only.

4.4 Coupling—field-test transmission performance

The waveguide joining imperfections comprise tilts, which result from both flange end-squareness deviations and coupling excess stiffness,

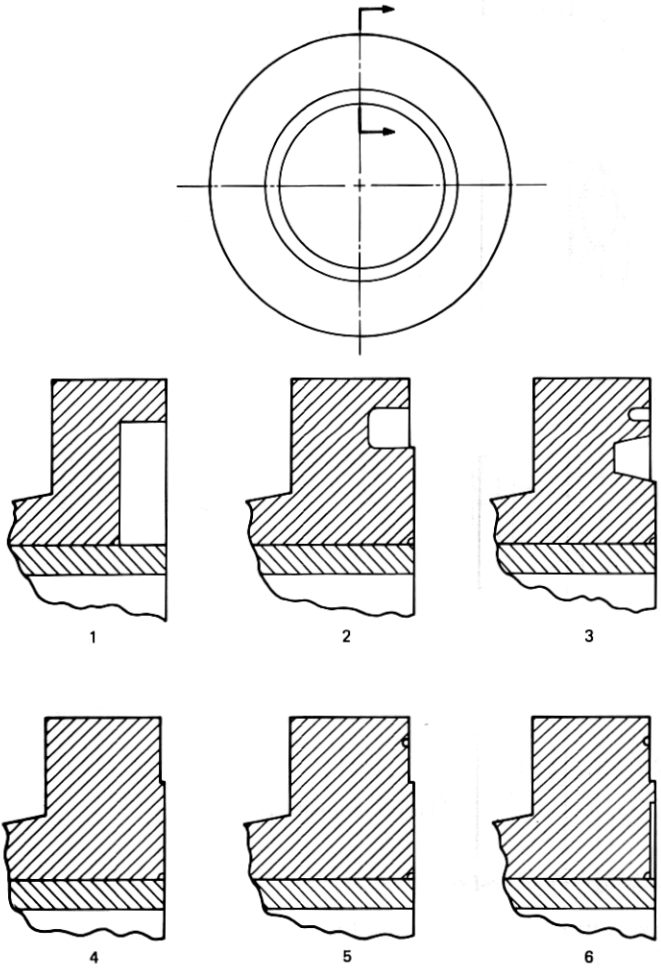

Fig. 12—Flange design stages.

offsets, which result from flange eccentricity and welder misalignments, and diameter distortions in the vicinity of the EB flange attachment welds. These imperfections resulted in a very small contribution to transmission losses in the field test waveguide.

Measurements of end squareness made on over 2600 flanges during Western Electric manufacturing indicated an RMS value of out-of-squareness of 0.064 milliradians. Assuming random joining of the flanges, the couplings would have an effective RMS tilt of 0.09 milliradians.

Thus for the waveguide medium, using eq. (10) with no interface gap assumed, the contribution to the net waveguide CPSD is

$$S_t(\omega) = 9 \times 10^{-10} \quad 1/\mathrm{m}^2/\mathrm{c}/\mathrm{m} \tag{13}$$

Table II — TIG nominal welding parameters

Current	170 amps
Voltage (dc)	16 volts
Welding time	95 sec
Overlap	10 deg
Argon-helium flow rate	15 CFH
Electrode	Thoriated tungsten, 0.093 in. diameter, 60 deg cone tip
Standoff	0.05 in.

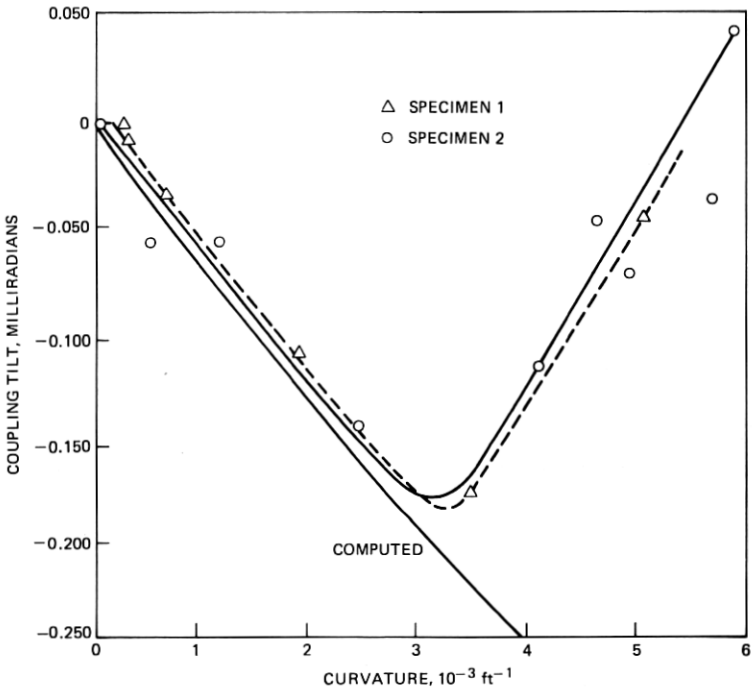

Fig. 13—Apparent tilt due to excess stiffness.

where the waveguide length is taken to be the nominal length of 29 feet. Since the loss is proportional to the square of the tilt, the reduction in tilt to 0.09 mrad from the initial objective of 0.2 mrad reduced the loss contributions of coupling tilt to one-fifth of that allocated.

The effect of excess stiffness of the coupling creates an "apparent tilt" when the waveguide is in a bend. The data in Fig. 13 indicate that the apparent tilt is a function of waveguide curvature. In the field test the RMS curvature of the waveguide in the vertical plane was about 1.33×10^{-3} ft^{-1}. This corresponds to an apparent tilt of 0.07 milliradians, a component almost as high as that resulting from the flange manufacturing irregularities.

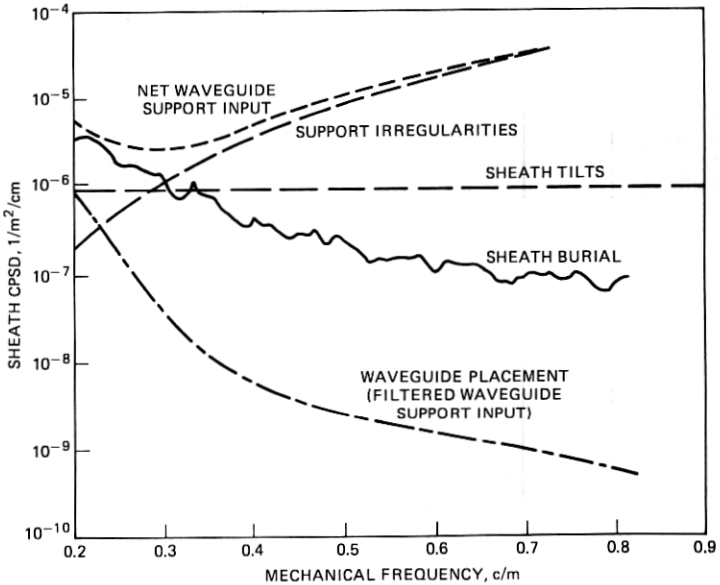

Fig. 14—Components of waveguide placement spectrum.

The offset caused by the eccentricity of the flanges as manufactured was negligible compared with the offset produced by the welder. The welder alignment fixture had a bias that contributed an offset of approximately 1 mil to each pair of flanges. This coherent bias of the welder, which could produce significant loss peaks, was mitigated by the rotation of the waveguide string during insertion. The waveguide string rotated slowly during insertion because of a slight canting of the roller axles in the supports. The potentially significant effects of radial distortions at couplings were removed by a randomization of module lengths.

V. SUMMARY

5.1 Loss contributions

The contributions to the net waveguide curvature of the various inputs associated with installation of the medium, in nominally straight regions, have been discussed in the preceding sections. As indicated earlier, waveguide axis curvature, including coupling tilts and offsets, is the only significant loss-producing effect of the assembly and installation of waveguide, the effects of diameter distortions at couplings having been made negligible by randomization of the waveguide lengths. (Ellipticity that results from bending the waveguide to the relatively large radii allowed is also negligible.)

In Fig. 14 the most important contributions to the net waveguide CPSD above 0.2 c/m are summed graphically. The sheath burial curvature is taken from the plot in Fig. 5. The other significant input contributions are the idealized estimates of support irregularities [eq. (9)] and sheath tilts [eq. (12)]. The squared transfer function for the waveguide support is that shown in Fig. 7. Adding the contributions of the sheath burial, sheath tilts, and support irregularities, one obtains the net WG-support input. Then, multiplying this result by the squared transfer function of Fig. 7, one obtains the waveguide placement spectrum. The expected value of the average combined TM_{11}, TE_{12} mode conversion loss corresponding to the waveguide placement spectrum is less than 0.06 dB/km at 110 GHz.

5.2 Conclusions

The field evaluation test results indicated that the basic objectives of the mechanical design of the sheathed waveguide transmission medium for the WT4 system were met. The field joining of waveguide for the field test was virtually trouble-free and, in addition, the remarkably high degree of machining accuracy achieved in the waveguide flange finishing was sufficient to limit this component of the loss budget to a nearly negligible level. The effectiveness of the mechanical filtering provided by the stiffness of the steel sheath and the action of the waveguide compliant support system permits installation of the sheath using the lowest-cost (conventional) methods of pipeline construction and eliminates the need for potentially troublesome expansion joints in the buried medium. The mechanical filtering is also sufficient to permit the use of pipe manufactured by commercial line-pipe suppliers and is tolerant of a reasonable degree of manufacturing imperfection in the supports themselves. Through use of relatively closely spaced compliant supports, the effects of waveguide weight and thermal loading distortions have been made negligible. The support developed for the field test is a low-cost reliable unit which, in addition to performing the filtering function, permits insertion of the waveguide in lengths of miles from a single point. Because of the substantial protection provided the waveguide by the rugged steel sheath, and the use of fusion joining of both the sheath and waveguide, the WT4 transmission medium is expected to be an order of magnitude higher in reliability than coaxial cable. As brought out by Alsberg et al.,[9] the installation method was carefully integrated with the overall system design[5,7] to achieve minimum costs.

VI. ACKNOWLEDGMENTS

Many people at both Western Electric and Bell Laboratories contributed to the development of the sheathed waveguide medium. Par-

ticularly notable contributions were made to the work reported on here by the following: P. L. Key, who was associated with the resolution of metallurgical problems on all of the elements of the sheathed medium; V. P. Chaudhary, who developed the finite difference solution and iterative procedure for the sheath-soil model; and P. M. Synefakis, who wrote the computer program for the sheath analysis and obtained the numerical results.

REFERENCES

1. R. J. Boyd, W. E. Cohen, W. P. Doran, and R. D. Tuminaro, "Waveguide Design and Fabrication," B.S.T.J., this issue.
2. D. J. Thomson, "Spectrum Estimation Techniques for Characterization and Development of WT4 Waveguide," B.S.T.J., this issue.
3. H. E. Rowe and W. D. Warters, "Transmission in Multimode Waveguide with Random Imperfections," B.S.T.J., *41*, No. 3 (May 1962), pp. 1031–1170.
4. J. W. Carlin and S. C. Moorthy, "Waveguide Transmission Theory," B.S.T.J., this issue.
5. J. C. Anderson, R. W. Gretter, and T. J. West, "Route Engineering and Sheath Installation," B.S.T.J., this issue.
6. M. G. Spangler, *Soil Engineering*, Scranton: International Textbook Co., 1951.
7. H. A. Baxter, W. M. Hauser, and D. R. Rutledge, "Waveguide Installation," B.S.T.J., this issue.
8. P. E. Fox, S. Harris, and D. J. Thomson, "Mechanical Gauging Techniques," B.S.T.J., this issue.
9. D. A. Alsberg, J. C. Bankert, and P. T. Hutchison, "The WT4/WT4A Millimeter Wave Transmission System," B.S.T.J., this issue.